# Correlating Multi-Phenomenology Measurements with Blast Design in a Copper Mine

Chris Hayward and Brian Stump, Department of Geological Sciences, Southern Methodist University
Mary A. Lowery, Phelps Dodge Morenci, Inc.

Blasting operations at one copper mine are studied in detail to examine the relation between blast design parameters and near-shot, in-mine, and regional seismic and acoustic observations. Five observational experiments, namely collection of blast design data, near source recordings, GPS synchronized video, near mine recordings and distant regional observations were performed during one week in August. A variety of seismic and infrasound instruments were installed near the shot, on the perimeter of the open pit mine, and at several locations up to 500 km distant. Time tagged video recordings were taken of several shots. Three shots were used in the preliminary analysis, a 350,000 lb pattern with long delays, a 60,000 lb pattern with short delays, and a 256,000 lb pattern with short delays. Maximum peak-to-peak amplitudes of the seismic signals in the mine are not a simple function of the total size of the shot, but are related to the pattern timing. Peak pressures have a less clear relation to peak pressure but match the relative amplitudes of spectra modeled from the pattern design. The predicted spectrum based upon a simple impulse model fits the observed spectrum for ground acceleration measured near the pattern and explains why in this case a pattern of 60,000 lb results in the same seismic disturbance as the 350,000 lb pattern.

## Introduction

This empirical study is part of a larger study designed to quantify mining explosion as sources of seismic and infrasound signals that may be recorded on stations associated with the Comprehensive Nuclear-Test-Ban Treaty monitoring network (Stump, 2001). In this study blasting operations at one copper mine are studied in detail using a network of near shot, near mine, and regional seismic and acoustic (infrasound) data recorders. Blasting operations in this mine account for 30% of all blasts observed and located by the USGS continental seismic network. Under optimal wind conditions, approximately 25% of the shots at the mine are observed on infrasound microphones as far 500 km away. Its been observed that the amplitude of distant seismic signals from this mine is not well correlated with the total explosive size of the blast. This paper illustrates the process with an in-detail examination of three instrumented shots.

## Data Acquisition and Experiment Design

During the week of Aug 6, 2001, five observational experiments were performed in the mine to determine how blast design is correlated with near and distant measurements of acoustic and seismic energy. During this time, four of the production shots were closely instrumented and photographed, but all shots had seismic and acoustic monitoring within several km of the shot.

Five observation experiments were done on each of four production blasts. The five observation experiments were the collection of blast design data, near source recordings, GPS synchronized video, near mine recordings, and distant regional observations. All instrumentation included GPS synchronized clocks such that observations could be precisely synchronized. Experiments were designed to use normal production blasts and to not interference with mine operations.

Blast design data of interest included the location, explosive weight, and timing of each borehole in the pattern. These design data were used in modeling seismic signatures and predicting the relative seismic amplitudes and spectra. Predicted detonation timing of individual holes was compared to the observations on the video and near source accelerometers to verify correct timing. Observations were made at three distance ranges (Figure 1), namely within 200 m of the pattern (near-source), around the perimeter of the pit (near-mine), and at regional distances of up to 500 km.

Four patterns were temporarily instrumented with various strong motion accelerometers and high-pressure microphones (Figure 2). Prior to each instrumented shot, two people spent about an hour to install four or five stations. Immediately after the shot, data was recovered and archived on CDROM. Exact recording parameters depended on the location, instrumentation, and purpose of the recording. Analog data was digitized on a 24-bit recorder between 250 samples per second (SPS) and 1000 SPS. Three sets of instruments were deployed. These were 1 g three-component accelerometers for installations at moderate distances (100m), 100 g three-component accelerometers for installations close to the shot (25m), and high-pressure infrasound pressure gauges for installation from 100m to several km from the shot. Infrasound gauges used in this experiment have a flat pressure vs. frequency response that extends from 1/10 to over 100 Hz.

Five near-mine locations within and on the perimeter of the mine were instrumented with longer term seismic and infrasound sensors (Figure 3). These recorders require about an hour each to install and record continuous seismic and infrasound data at 40 SPS. During large signals, they trigger a 250 SPS high frequency recording. Recorders are self-powered, self-contained and require no maintenance other than a visit once every few months to exchange disks. One location, near the center of the mine, includes three acoustic gauges in a small array and a broadband three-component seismometer. These recorders collect seismic and acoustic information for every significant blast in the mine during the several month observation period.

Several long term infrasound arrays and seismic stations have been installed (Figure 4) up to 500 km from the mine. These stations include four infrasound microphones arranged in a small array that may be beam steered to focus on particular directions. Distant stations can use the array to determine a signal's arrival direction and to discriminate between signal and wind-generated noise. The stations are similar to the near-mine stations in that they are self-contained and require a visit every few months to recover the data.

For each on the instrumented shots, two GPS locked video cameras were installed at overlooks (Figure 5). These are standard High-8 video cameras that are synchronized to a GPS timing signal and to each other. After post processing, there is one time tagged frame recorded every 16 milliseconds. Since the cameras have a recording capacity of two-hours there is ample time to setup and start video prior to the shot.

## Analysis

We focus on three shots in this preliminary analysis (Figures 6 and 7). Two of these occurred August 6, a long duration shot 325,000 lb shot with extended delays and 35 seconds later a smaller 60,000 lb shot with short delays. A third 256,000 lb shot with short delays was recorded August 8. The in-mine vertical velocity waveforms (Figure 8), acoustic pressure (Figure 9) and spectra (Figure 10) illustrate the kind of information collected for each blast in the mine. Seismograms and infrasound recordings (Figures 8 and 9) are organized in order from closest to furthest. The station OLD402 is the closest to each shot. The station BONEYARD is furthest from the shot. Maximum velocity and pressure are indicated above each waveform. Since shots 1 and 2 are nearly in the same location, amplitude distance corrections to the four stations should be about the same. The peak amplitudes recorded on the first shot at the in-mine stations are from 3 to 1.2 times as large as those from the second shot. Amplitudes for all three shots decay with the increasing distance.

Recorded acoustic waveforms are simpler along the time axis, but have a less predictable amplitude pattern. For example, site OLD402 shows almost the same acoustic peak pressures (about 18 Pa) for both blasts even though the second blast is only about 1/6 the size as the first blast. Site NEW402 is about one-half the amplitude on the second shot, while site 35SUB is over 4 times larger for the second smaller shot than the first shot. The period of the acoustic waveform appears to be related to the total duration of the mass movement, about 5 seconds for the first shot and about 3 seconds for the third shot. Video of the second shot was obscured by the first shot. In Figure 10, spectra for seismograms and pressure signals from site OLD402 are compared. Below 5 Hz, shot 3 is the most energetic. The shot with the largest amount of explosives (Shot 1) produces the smallest amplitudes at mid periods but dominates at high frequencies. These data suggest complicated amplitude scaling for both the seismic and acoustic signals.

Design delay times for the three shots were used to produce an impulse series representation of each shot (Figure 11). A spike was positioned at each of the design detonations. The height of the spike indicates the number of holes detonated at each time instant. The spectra of the signals are shown on the right of Figure 11. As in the observations, Shot 3 has the largest amplitudes at low frequencies. The model spectra suggest that the complex interaction of intershot delay patterns and total source duration can reduce amplitudes in the 1-10 Hz frequency range by over an order of magnitude. The spectra of the shot patterns compare well with the displacement spectra determined from near-field acceleration measurements for each shot (Figure 12). Note that synthetic spectra and observed spectra for site match well for site OLD402, further supporting the importance of shot timing on the radiated waves. Above 10 Hz, the assumption of an impulse to represent each shot is an oversimplification and observed and theoretical spectra are expected to diverge. The model suggests that the largest shot may product the smallest amplitudes at distant seismic stations where signals are typically recorded in the 1-5 Hz band.

Figure 13 shows a seismogram recorded at Tucson for shots 1 and 2. The shots were separated by about 35 seconds. Note that as predicted by the model, the two blasts are approximately the same amplitude at Tucson even though the first blast is nearly 6 times the size of the second.

## Conclusion

There is a complex relation between seismic and acoustic amplitude and total blast size that is a complex function of the pattern timing. Models are successful in predicting relative amplitude differences in the seismic amplitudes, but do not explain all the differences in the acoustic amplitudes. High frequency amplitudes observed at regional seismic stations support the in-mine and modeled observations.

## Acknowledgements

A number of individuals at Phelps Dodge mines, the US National Park Service, the Texas General Land Office, and Southern Methodist University have made the data acquisition possible through their assistance with planning, installation, field acquisition, and daily operation. The project was sponsored by the Defense Threat Reduction Agency under contract DSWA01-98-C-0176.

## References

Stump, Brian (2001); Chris Hayward; Claus Hetzer; and Rong-Mao Zhou. Utilization of Seismic and Infrasound Signals for Characterizing Mining Explosions in Proceedings of the 23rd Seismic Research Review: Worldwide Monitoring of Nuclear Explosions – October 2-5, 2001. National Nuclear Security Administration LA-UR-01-4454.

## Illustrations

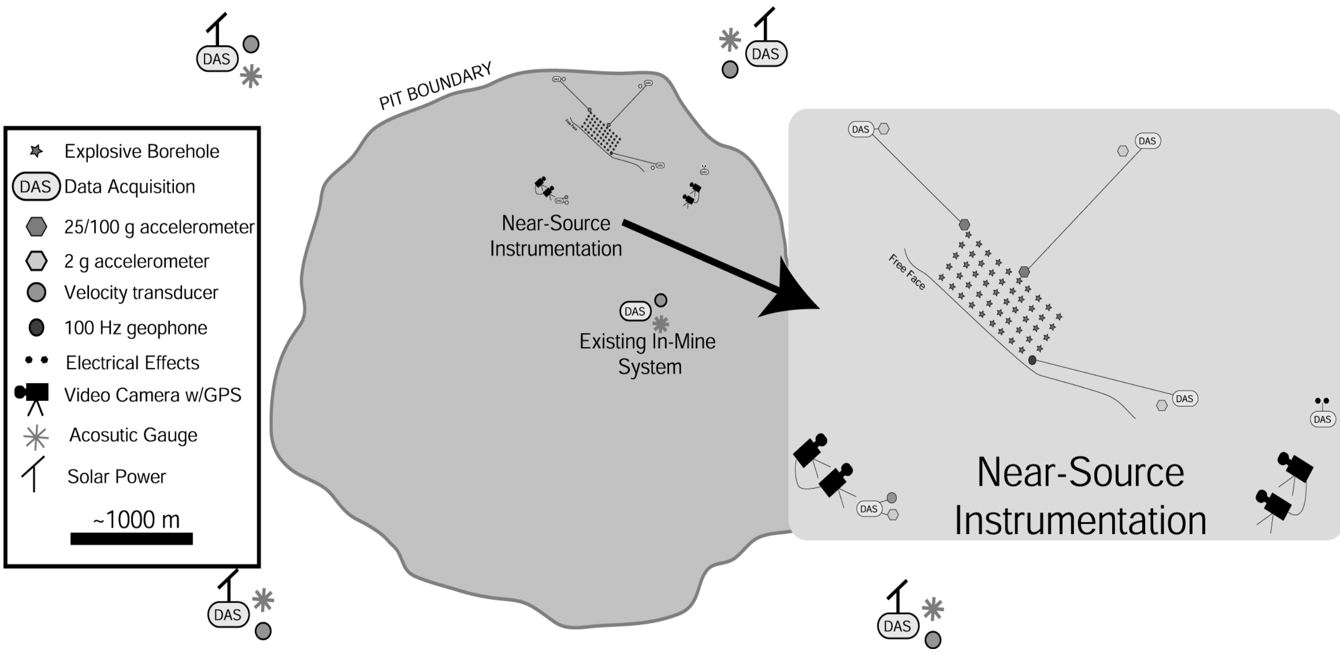


Figure 1. The instrumentation includes temporary near-source seismic, acoustic and video recorders (on right inset) and additional long-term seismic and acoustic recorders on the perimeter and center of the pit. Each system is self contained, can run unattended and is locked to GPS time and records a GPS location.

Figure 2. Two people install one of the four near shot monitoring stations. This station includes two three channel recording systems running at 1000 samples/second continuous recording output from a 3 component 1 g accelerometer and a 25 g accelerometer. The pattern is just below the hill in the background.

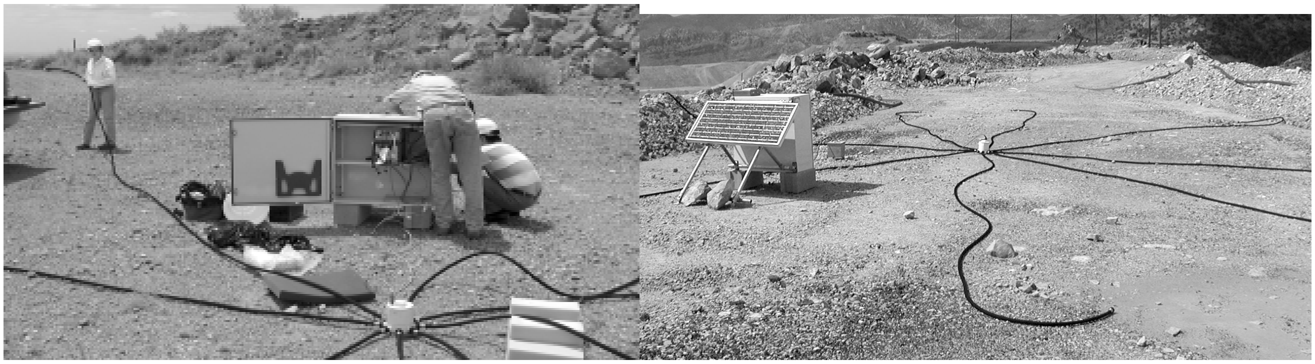

Figure 3. On the left, three people are setting up one of the long-term temporary in-mine seismic and infrasound recorders. The sensor in the front is the infrasound sensor with porous hose wind noise suppressor. Installation of such a system requires about an hour. On the right, the recorder is shown after installation. The seismometer is the small gray box between the infrasound gauge and the solar power system. The in-mine recorder is solar powered and completely self-contained. It records about two months of continuous 40 SPS seismic and infrasound data internally on a disk. In addition, large signals, such as blasts, trigger a high frequency recording at 250 SPS.

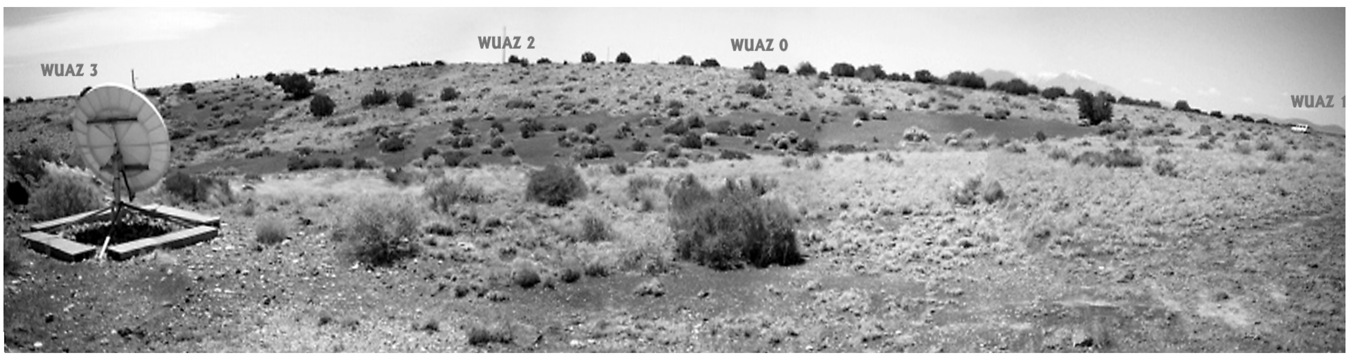


Figure 4. This station is near Flagstaff, Arizona and includes four separate infrasound microphones arranged in an array. Microphones locations are below the various WUAZ labels in the photography. The satellite antenna is used to telemeter seismic data to the USGS National Seismic Network where it may be retrieved by researchers in near real time. The infrasound data is recorded on a self-contained system similar to Figure 3. Two people can install such a system in one work day. Besides locating and identifying mining explosions several hundred km away, such systems can also identify large meteors, sonic booms, some aircraft, rockets, and other kinds of accidental explosions (factory, gas lines).

Figure 5. GPS locked stereo video camera recorders are setup at a convenient location with a good view of the shot. The cameras are synchronized to each other and to GPS time. These are standard video cameras and after post processing, one frame is produced each 16 ms fom each camera. The use of two cameras gives additional redundancy and can provide stereo images of the shot.

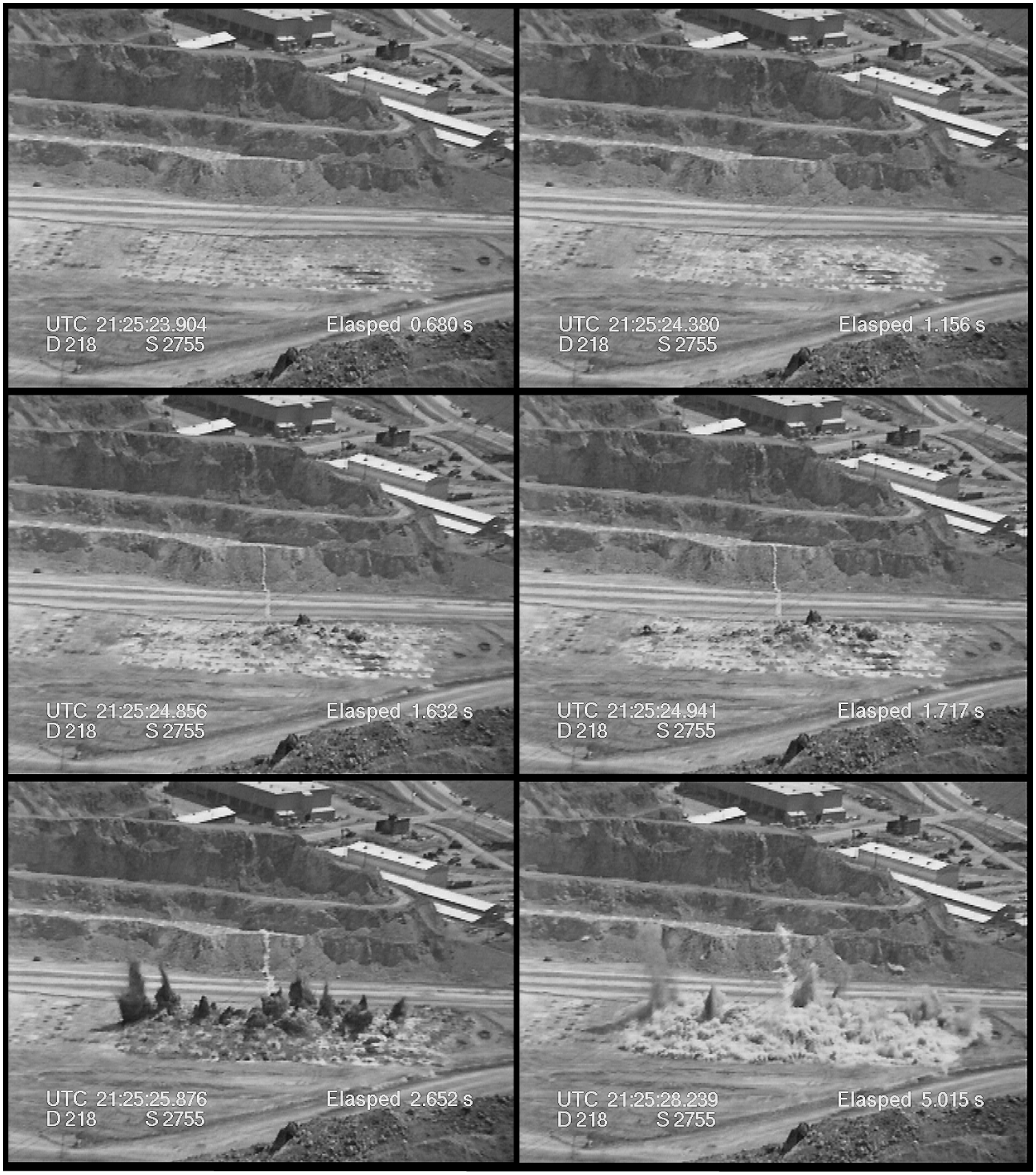


Figure 6. Six selected frames sequenced left to right, then top to bottom have been extracted from the video recordings. Elapsed time begins upon shot. A brief flash at each hole confirms hole detonation. Maximum vertical displacement occurs 2.5 s after initiation and rejoin occurs at 4.0 seconds, yielding a maximum vertical displacement of approximately 10 meters. The shot has delays of 67 to 100 ms and a total explosive weight of about 350,000 lbs. A second smaller pattern (about 60,000 lbs) is directly behind the main pattern on the first bench. Seismic and acoustic waveforms from these two shots are shown in the following figures.

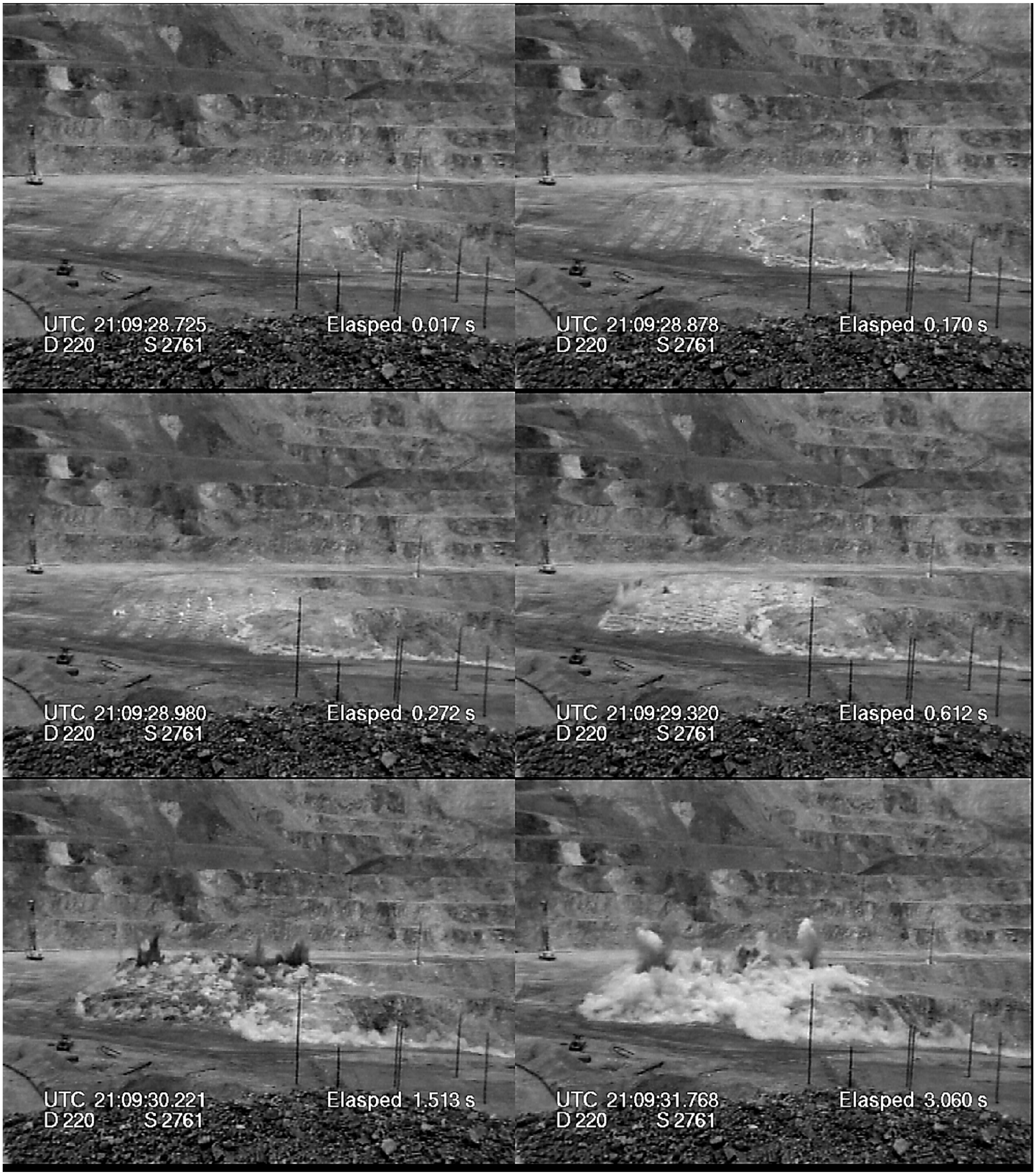


Figure 7. This sequence of six frames is taken from the third shot, a 256,000 lb with delays from 17 to 42 ms. The maximum vertical rise occurs at 1.5 seconds and mass rejoin occurs at about 3 seconds. Seismic and acoustic waveforms recorded from this shot are shown in the following figures as the third sequence of waveforms. Compare the timing on this shot with the one in figure 6, a shot of similar size.

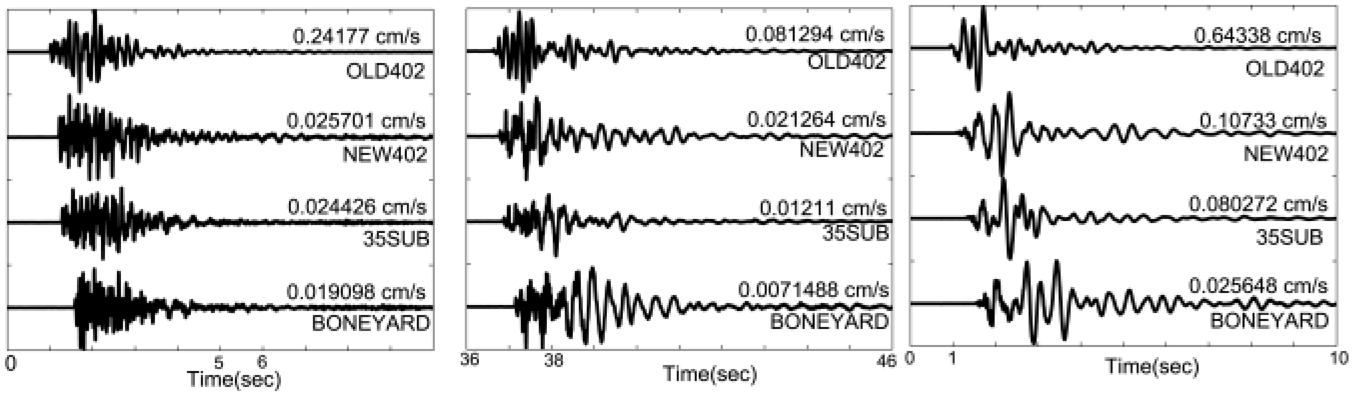


Figure 8. The seismic waveforms from the three shots mentioned in figures 6 and 7 are shown above. From left to right, the waveforms show the 350,000 lb shot, the 60,000 lb shot and the 256.000 lb shot. Following figures have this same order. The maximum velocity as measured on the 2 Hz seismometer is displayed on each figure along with the station name.

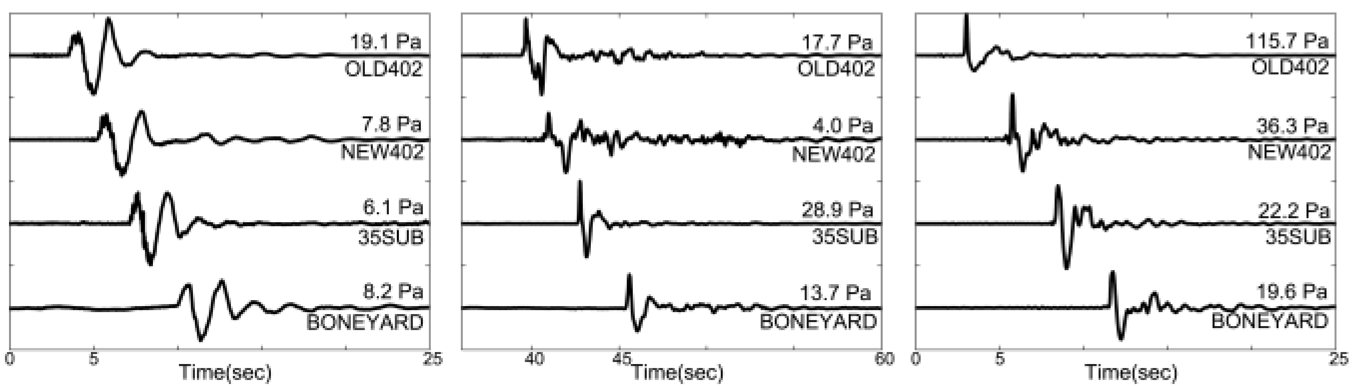


Figure 9. The waveforms in the above figure are the infrasound (acoustic) measurements corresponding to the seismic waveforms in figure 8. Like the previous figure, the waveforms are organized from near to far for each shot. The time scale is much longer here (5 seconds between tick marks) to allow for the much slower velocity of sound in air. In contrast to the seismic recordings, the acoustic waveforms do not always show a strict amplitude decay with distance, probably the result of topographic shadowing.

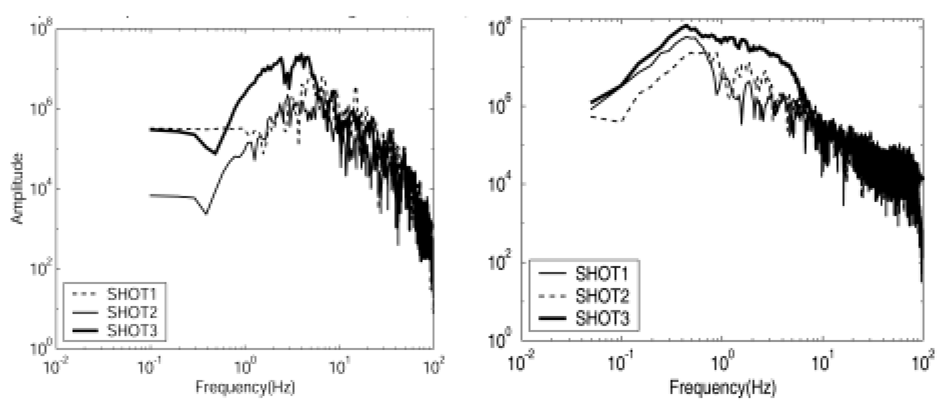


Figure 10. The two figures above show the power spectra for the three shots recorded at site OLD402, the closest of the perimeter stations and the station with the largest signal. The spectra on the left are for the seismogram and that on the right are for the pressure signals. Compare the spectra for shots 1 and 3 (the two shots about the same size).

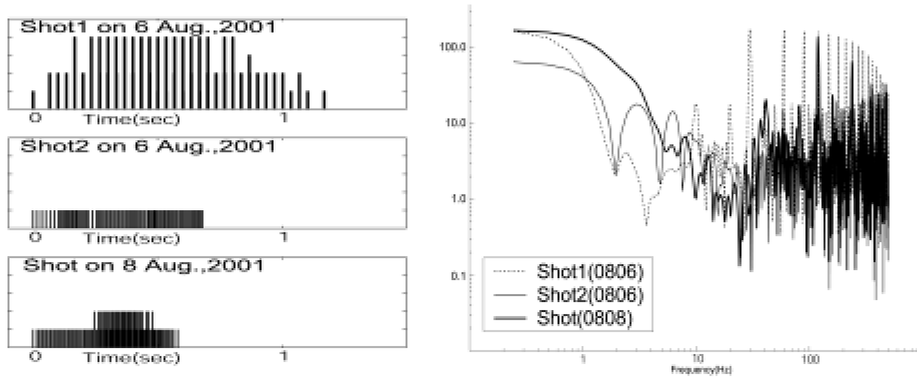


Figure 11. On the left, a synthetic impulse response is constructed for the three shots. The sequence consists of one impulse located at the design detonation time for each shot. The heights of the spikes indicate the number of holes that will be detonating simultaneously. On the right, the power spectra is shown for each of the synthetic impulse responses. Of particular interest is the shape of the spectra between 0.5 Hz and 10 Hz. Spikes at high frequencies result from evenly spaced delays and probably are likely suppressed in any realistic shot.

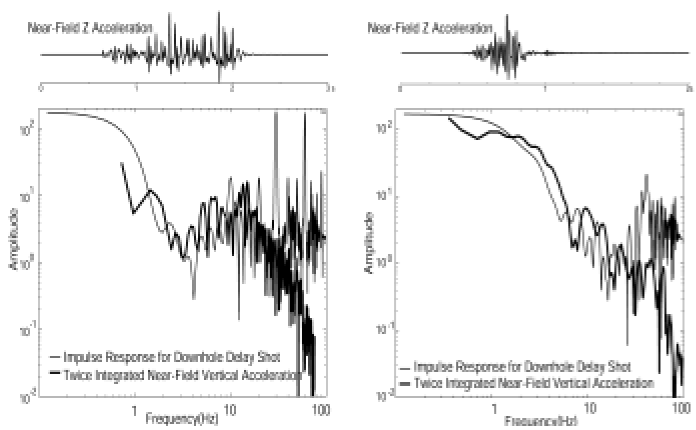


Figure 12. On the left is the observed acceleration observed close (100m) to the first shot (figure 6). On the right is the observed acceleration for the third shot (figure 7). The time scale has been expanded slightly on the right. Below each waveform plotted as a heavy line are the power spectra of the waveform and as a light line the theoretical power spectra. Divergence above 20 Hz probably results from the frequency response of the individual shots in the pattern rather than a problem with the theoretical fit.

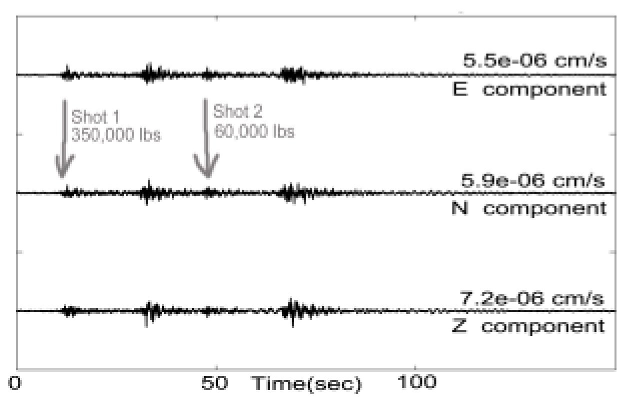


Figure 13. The seismograms above show the signals from the first two shots as recorded at Tucson, Az. Note that the two shots while differing in size by 6 times, result in seismic signals that are nearly the same size. This is consistent with the spectra recorded on the perimeter seismic stations (figure 8) that indicate that above 1 Hz, the two signals have similar power.